How graph structure and connectivity affects the propagation of cooperation in a network

Laura Koemmpel, Olga Medrano
Mentored by Ashwin Narayan
Project suggested by Ashwin Narayan

August 2, 2018

Abstract

The notion of cooperation in biological systems has recently motivated the formation of *evolutionary game theory*, the study of evolving populations through game theoretic methods. Through modeling individuals as nodes in a graph and connections between them as edges, evolutionary game theory focuses on the dynamics of *node strategy updating*. This consists of nodes changing their strategies or behaviors according to a given process in either a discrete or continuous time basis. In this paper we study the long-term behavior of graphs with highly interconnected and highly sparse regions (such as the *two-island*, *two-barbell*, and *rich-club* graphs) under the *birth-death* and *death-birth* reproduction models given a *prisoner's dilemma* payoff matrix. We discuss empirical evidence and observe that the *degree-weighted frequency difference between two cliques* tends to zero after long periods of time through observing the expectation of its derivative.

Contents

1 Motivation

A central notion that has been of interest to game theorists and biologists for decades has been that of *cooperation*, which is defined to be the action of helping or bestowing some benefit upon another individual. Cooperation usually requires an individual to pay some sort of personal price, and with no guarantee their neighbors will reciprocate their generosity, the simple fact that an individual will cooperate at all is an intriguing one. After all, why should an individual as seemingly insensate as a bacterium care to help one of its competitors in the struggle for survival? Nevertheless, cooperation does occur, and this kind of behaviour has been present in several milestones of life on Earth [5], such as the formation of multicellular organisms or the organization of living creatures into communities. Game theory has provided a useful way to approach these kinds of questions, however many of its intricacies have yet to be fully explored.

As for the field of *noncooperative game theory*, it primarily focuses on games or dilemmas that are to be played just once and in which all players behave with complete rationality; this means it is assumed that players know the rules of the game and all data about other players [7]. However, although many organisms lack the ability to make rational decisions, in general, their behaviour still adheres to some of the principles of noncooperative game theory, such as the fact that the outcome of the individuals' decisions depends on a payoff matrix. A popular example of this is that of bacteria; although they lack the ability to remember past events and improve their way of approaching situations based off of that knowledge, they can still make decisions which lead to symbiotic relationships. Some years ago, a study [8] observed four different species of bacteria all coexisting on the tomato plant in order to promote the plant's growth through hormones and to prevent the growth of hostile bacteria.

Evolutionary game theory (EGT) serves to model these situations with games that are played over and over. Individuals are chosen from the population according to some stochastic process in order to interact or reproduce a copy of themselves accordingly, although still not necessarily in a fully rational way [7].

Such models can help us to better understand the evolution and propagation of certain behaviors in a network, such as cooperativity or even a mutation in a gene. What's more, the results in this area can be applied to various real-world situations, such as the spread of cancerous cells and the response of a tumor to therapy [6], or the spread of an emotion through a massive social media network such as Facebook [3].

1.1 Evolutionary mechanisms

EGT has led to the study of different mechanisms for determining the way in which a game develops, such as how nodes receive their payoff or reproduce [5]. Some mechanisms require that the individuals have memory of past occurrences and others do not. Two evolutionary mechanisms of main interest are *fitness-based assessment* and *spatial selection*.

Fitness-based assessment consists of each individual taking action according to its level of fitness, or to the fitness level of its adversary; note that fitness, though not rigorously

defined yet, is a measure of reproductive ability. In short, it tells how well a node is doing at the current point in time with respect to the network that it's in. *Spatial selection* is a mechanism in which network structure is a strong factor in determining who interacts with whom and who competes with whom in order to reproduce. The graphs that determine reproduction and interaction need not be the same, nor must they have static structure [5]. However, in this work we assume both graphs are static and coincide.

As an alternative for *fitness-based assessment*, an individual can decide its action by assessing its own strategy, i.e. decision making process. One strategy that is commonly modeled in evolutionary game theory research is *tit-for-tat*, in which the player cooperates in all its first encounters with others and from then on replicates the action of its latest opponent. The main focus of this work is on the strategies *always cooperate* and *always defect*. In particular, we explore how the proportions of individuals with a particular strategy can evolve over time, and we attempt to determine what the long-term steady state proportions of cooperators are for various graphs.

2 Setup

We now study how a strategy can propagate through areas of a graph. We therefore give special attention to the role of network structure in the evolution of cooperation through EGT models. In evolutionary games, we are interested in interactions between individuals, each of which can decide between cooperating or defecting (helping or not helping the other). These interactions take place between pairs of individuals in a population represented by a graph, comprised of the following elements:

- **Nodes** represent individuals from a population
- An **edge** between two nodes indicates that these are neighbors and have some probability of interacting with each other.
- **Edge weights** represent the propensity for two neighboring nodes to interact.

After the graph is defined, it follows an evolutionary game. At each timestep we have the following:

1. Some pairs of nodes interact (simultaneously or not), and parameters in the graph are updated accordingly
2. A node reproduces itself by copying its own strategy and replacing that of another node

2.1 Graph-structural definitions

Since every edge has a given weight, and these weights will affect the likelihood of certain events to happen, we define several variables which will be necessary later on.

Definition 2.1. A *network* is a graph $\mathcal{G}(V, E)$, consisting of a set of vertices V and a set of undirected edges E.

Remark. Throughout this paper, all networks are assumed to be connected, nonbipartite, undirected and with no self loops.

In a graph as defined above, we use w_{ij} to denote the **weight of the edge** that connects $i, j \in \mathcal{G}$. Since $\mathcal{G}$ is undirected, then $w_{ij} = w_{ji}$. These variables let us define **node weights**, $w_i = \sum_{j \in \mathcal{G}} w_{ij}$; thereupon we can define the **total graph weight**, $W = \sum_{i \in \mathcal{G}} w_i$.

If we were to perform a random walk on $\mathcal{G}$, with steps taken with probability proportional to edge weight, then the probability to take a step from node i to node j is $p_{ij} = \frac{w_{ij}}{w_i}$. Then, the probability that an n step walk starting from i ends up at j is $p_{ij}^{(n)}$. We know that, since $\mathcal{G}$ is connected and nonbipartite, there is a unique stationary distribution $\{\pi_i\}_{i \in \mathcal{G}}$ for this random walk, in which $\pi_i = \frac{w_i}{W}$.

As a last note in this section, we provide the following result, which will be needed in order to do some of the substitutions later on in Section 4.

Proposition 2.1. *Given the previously defined variables,* $\pi_i p_{ij} = \pi_j p_{ji}$

Proof. We can note, by the definitions above that

$$\frac{\pi_i}{\pi_j} = \frac{w_i/W}{w_j/W} = \frac{w_i}{w_j}$$

On the other hand,

$$\frac{p_{ji}}{p_{ij}} = \frac{w_{ji}/w_j}{w_{ij}/w_i} = \frac{w_i}{w_j}$$

Therefore, $\frac{\pi_i}{\pi_j} = \frac{p_{ji}}{p_{ij}}$, and we conclude the proof.□

2.2 Pairwise interactions

Remark. In our interaction model (*death-birth*, which we explain thoroughly later on), our nodes take decisions based off in one of the strategies *always-cooperate* or *always-defect*. We declare then, for each $i \in \mathcal{G}$, a strategy variable s_i which takes the value 0 or 1, respective to the strategies previously mentioned.

Definition 2.2. Given two individuals $i, j \in \mathcal{G}$, a *pairwise interaction* is given by a game in which each of the individuals can decide between cooperating (C) or defecting (D).

Definition 2.3. Given a pairwise interaction, its *payoff matrix* is a 2×2 matrix whose entries determine the payoffs for each of the involved players, correspondingly.

Remark. We are assuming that the payoff matrix is symmetric; this means that if the payoff matrix for the first player is:

$$M = \begin{array}{c} \\ C \\ D \end{array} \begin{array}{c} \begin{array}{cc} C & D \end{array} \\ \begin{pmatrix} R & S \\ T & P \end{pmatrix} \end{array}$$

then the payoff matrix for the second player is M^T.

Definition 2.4. A pairwise social dilemma with strategies C and D is called a *prisoner's dilemma* when $T > R > P > S$

Remark. In other words, a game is a prisoner's dilemma if it is always best for a player to defect, regardless of the other player's action.

Definition 2.5. The *donation game* is a prisoner's dilemma game whose payoff matrix for the first player is:

$$M = \begin{array}{c} \\ C \\ D \end{array} \begin{array}{c} \begin{array}{cc} C & D \end{array} \\ \begin{pmatrix} b-c & -c \\ c & 0 \end{pmatrix} \end{array}$$

. The payoff matrix for the second player is M^T, with $b > c$. We call **b** the benefit and **c** the cost of the donation game.

Remark. In other words, a donation game is one in which each player can either *cooperate* (paying cost c and generating a benefit of b for its partner), or *defect* (not paying any cost, although still accepting benefit) under the condition $b > c$. As a result, mutual cooperation generates $b-c$ for both players, mutual defection generates 0 for both players, and cooperation-defection generates b for the defector and c for the cooperator.

Definition 2.6. In the game above, the *benefit to cost ratio* is defined as b/c.

Remark. As has been worked with in previous papers [2], [1], we may perform a change of scale in the payoffs of the game above and assume $c = 1$.

2.3 Reproduction variables

Another important aspect of evolutionary games is that of strategy propagation. We define here some of the variables pertinent to the *death-birth process*, whose guidelines we specify later in section 2.

Definition 2.7. We define $\mathbf{f_i(s)}$ to be the **edge-weighted average payoff** of vertex i in state s. This value depends on the states of i's neighbors, the payoff matrix for the graph, and the probability of i interacting with its neighbors, and has the following form:

$$f_i(s) = -cs_i + b\sum_{j\in\mathcal{G}} p_{ij}s_j$$

Definition 2.8. We define $\mathbf{F_i(s)}$ to be the **reproductive rate** of vertex i given state s. $F_i(s)$ can be expressed as $F_i(s) = e^{\delta f_i}$ or, assuming δ is very small, we may take the Taylor expansion and express $F_i(s)$ as

$$F_i(s) = 1 + \delta f_i$$

.

Definition 2.9. We define δ to be the **strength of selection**. This is a factor affecting the degree to which node fitness levels affect their ability to reproduce.

2.4 Recent result

A recent paper from Benjamin Allen *et al* (2017) [4] proves a strong technique that determines whether any given network structure favors cooperation or not under weak selection using the following notation and propositions:

Definition 2.10. We define ρ_A as the probability that a node with interaction strategy A emerging at a random place in $\mathcal{G}$ takes over the population.

Proposition 2.2. *A network structure $\mathcal{G}$ following the donation game favors cooperation when $\rho_C > \frac{1}{N}$, where N is the number of nodes in $\mathcal{G}$.*

Proposition 2.3. *A network structure $\mathcal{G}$ following the donation game favors cooperation when $\rho_C > \rho_D$.*

Remark. The propositions above are equivalent when players interact through a donation game.

This paper uses a duality between the probability that two coalescing random walks meet at time $t < T$ and two nodes having the same strategy after T steps of reproduction of the evolutionary game. Then, for any network we can calculate $\left(\frac{b}{c}\right)*$, where:

Definition 2.11. The *critical benefit to cost ratio*, or $\left(\frac{b}{c}\right)*$ (when it is positive) is the amount such that natural selection favors cooperation in the given network whenever the benefit to cost ratio is greater than the given amount.

Remark. It always happens that $\mid \left(\frac{b}{c}\right)* \mid > 1$.

Remark. When $\left(\frac{b}{c}\right)*$ is negative, then natural selection inhibits cooperation regardless of the benefit to cost ratio.

Then, the closest that $\left(\frac{b}{c}\right)*$ is to 1 (given that it is positive), the better that the graph is in promoting cooperation.

2.5 Models

We considered connected, nonbipartite, undirected graphs $\mathcal{G}$ with no self loops and with edge weights $w_{ij} = w_{ji}\ \forall i, j \in \mathcal{G}$. We carried Monte Carlo simulations on these graphs, where in each timestep we updated the graph according to the guidelines below, in the following order:

1. A reproductive step, which could follow one of the two following models:
    - *Death-birth*: $j \in G$ is chosen uniformly to be replaced, and a node $i \in G$ is chosen among j's neighbors, with probability proportional to $F_i w_{ji}$. Then, i replaces the node j.
    - *Birth-death*: $i \in G$ is chosen with probability proportional to F_i, and then one if its neighbors $j \in G$ is chosen uniformly at random. Then, i replaces the node j.

Both of these models, however, do not alter the graph's structure, i.e. the connections or edge weights of the replaced node are left unchanged.

2. An interaction step, in which every pair of nodes interact through a prisoner's dilemma game, where each node can either cooperate or defect, and the payoff for the first player is given by the following payoff matrix

$$\begin{array}{c} \\ C \\ D \end{array} \begin{array}{c} \begin{array}{cc} C & D \end{array} \\ \begin{pmatrix} b-c & -c \\ 0 & b \end{pmatrix} \end{array}$$

Each of the two players decides whether to cooperate or not in the following way:

- *By strategy:* We have only two strategies in our model, *always-cooperate* and *always-defect*. Then, if i and j interact with each other, then i's intended action is cooperating iff $s_i = 1$, which corresponds to the strategy *all-cooperate*.

Furthermore, we included the following factors which could add *noise* to our simulations:

- *Mutation:* When node i with strategy s_i makes a copy of itself whose strategy is $\widetilde{s_i}$ and replaces some other node j, there is some probability that the replication is not exact, in the sense that $s_i \neq \widetilde{s_i}$. We denote the probability of this happening (in any reproduction event) as $u \in [0, 1]$
- *Noise:* When node i interacts with node j, and has intention of action $a_i \in \{C, D\}$, we denote $p_{\text{noise}} = \mathbb{P}[\overline{a}_i \neq a_i]$, where $\overline{a}_i$ is the executed action by i.

Remark. In the *death-birth* model, the probability that i replaces a node j, given that j is going to be replaced, or Rate$[i \to j]$, is

$$\text{Rate } [i \to j](s) = \frac{w_{ij} F_i(s)}{\sum_{k \in \mathcal{G}} w_{kj} F_k(s)}$$

3 Empirical Work

Accurately modeling a network of many players interacting simultaneously and updating their strategies is computationally intense, so to discover the long-term behavior of such a network we turn to empirical simulations. In such simulations we may explore how varying the structure, connectivity, and starting proportions of cooperators in a network affects it's long-term steady state.

In order to further understand how strategies may propagate from one highly connected group to another, we focus our simulations on modelling barbell, island, and rich club graphs. Throughout our simulations, we fixed the following parameters for mutation, strength of selection, benefit and cost values, and noise probability, respectively:

$$u = 5 \times 10^{-5} \qquad \delta = 0.002 \qquad b = 2 \qquad c = 1 \qquad p_{\text{noise}} = 5 \times 10^{-5}$$

3.1 Barbell graphs

Although there are several conventional definitions for the barbell graph, in this work we consider a **2-barbell graph**, with the following definition:

Definition 3.1. A **2-barbell graph** is a graph consisting of two fully connected cliques joined by a path of length n between two nodes, one from each clique.

Figure 1 shows an example of a 2-barbell graph with a connecting path of length 2.

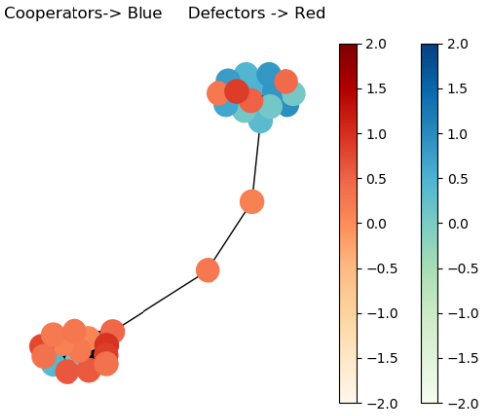

Figure 1: A two-clique barbell, with 20% and 70% cooperators in each clique. Color intensities denote fitness levels, which are randomly chosen at the initial state which is shown here.

One of the unique structural aspects of barbell graphs is their propensity for protecting cooperators. Considering the case of a complete clique with N nodes, its value of $(b/c)^*$ is negative, implying that this graph does not promote the diffusion of cooperators. However, if our scenario consisted of two cliques (each of size N) which we connect through a pair of nodes (one representative in each clique), then $(b/c)^*$ becomes positive and finite, albeit growing quadratically with respect to the number of nodes, namely at a rate of $\mathcal{O}(N^2)$. In other words, connecting two communities that don't promote cooperation might result in a new graph that does promote cooperation [2].

Another structural aspect of barbell graphs is that they have the potential to create a bottleneck for strategy propagation. For example, suppose a network was modeled by a 2-barbell graph in which one clique (call it clique $\mathcal{A}$) starts with all nodes cooperating and the other (call it clique B) starts with all nodes defecting. Aside from variations due to mutation and noise, the only way for B to gain a cooperator node is for a cooperating node of $\mathcal{A}$ to reproduce and replace a path node, that path node to then in turn reproduce and replace its neighboring path node, and so on, until finally a cooperating path node can reproduce its strategy onto $\mathcal{B}$. We supposed that when clique sizes are small, sequence of actions would be somewhat probable, as is supported by the simulation data in figure 2.

We also supposed that when the clique size increases it becomes much harder for cooperators propagating into the defector clique to survive. If a cooperator is born into

a very large defector clique it will most likely be exploited by its neighbors until its fitness level lowers to the point that it dies off. This leads to both cliques retaining their proportions of cooperators close to their initial states, as is supported by the simulation data in figure 3. However, for many trials, the data is not so intuitive. Often proportions of cooperators in cliques remain different from each other, even with clique size is small.

Note that for all simulations of barbell graphs we employ the *birth-death* model for strategy updating.

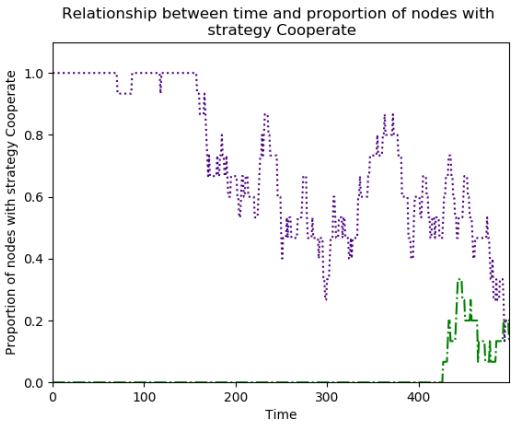

Figure 2: Above we see the proportion of cooperators over time for each clique in a 2-barbell with cliques of size 15, an intermediary path of length 4, and each clique starting with either all cooperators or all defectors. The different cliques are denoted by the differently colored and styled lines.

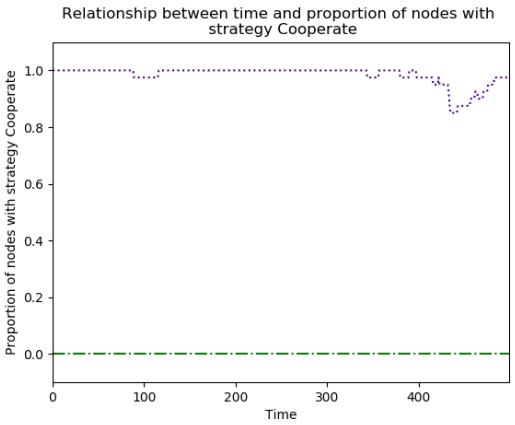

Figure 3: The proportion of cooperators over time for each clique in a 2-barbell with cliques of size 40, an intermediary path of length 4, and each clique starting with either all cooperators or all defectors. The different cliques are denoted by the differently colored and styled lines.

In figure 4, we graph the proportions of cooperators over time in each clique of a 2-barbell when one clique begins with ten percent of its nodes having the strategy cooperate and the other begins ninety percent of its nodes having the strategy cooperate. Over time we can see that the proportions of cooperators in each of the nodes become equal. This can be seen more clearly in figure 5, which plots the difference between proportions of cooperators in each clique of the barbell. However, in other trials, the difference in proportions of cooperators remains different, even across long periods of time, as we can see in figures 6 and 7

To formalize this discrepancy we graph the average of many trials with the same parameters in figure 8 and see that over time the standard deviation across trials becomes very high. Therefore our empirical data cannot be considered conclusive, and so in order to understand the propagation of strategies more precisely, we turn to other graph structures, as well as theoretical calculations for a graph's steady state.

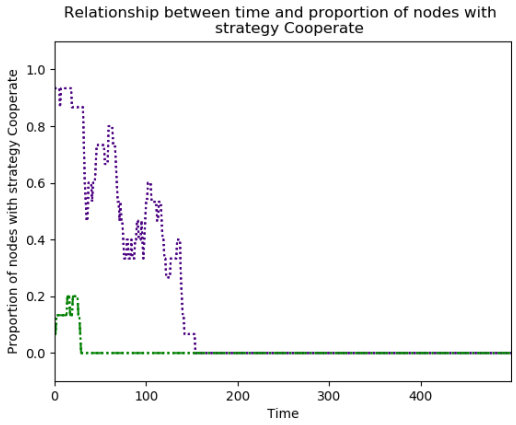

Figure 4: The proportion of cooperators over time for each clique in a 2-barbell with cliques of size 15, an intermediary path of length 4, and each clique starting with either 10% or 90% cooperators. The different cliques are denoted by the differently colored and styled lines.

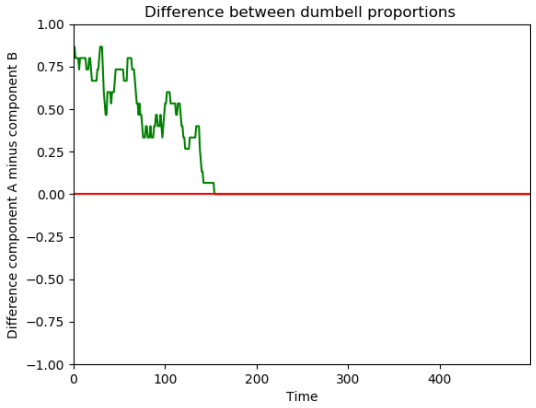

Figure 5: Difference in proportions of cooperators for a two-clique barbell graph with cliques of size 15, an intermediary path of length 4, and each clique starting with either 10% or 90% cooperators.

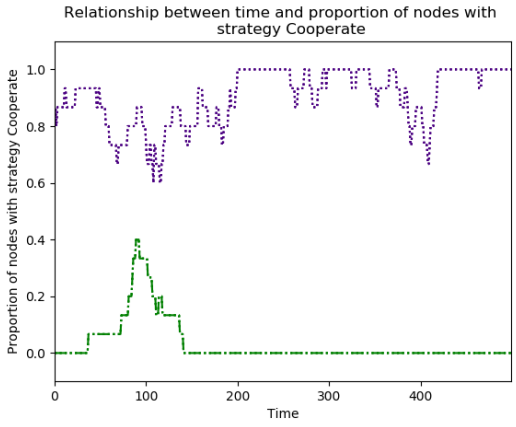

Figure 6: The proportion of cooperators over time for each clique in a 2-barbell with cliques of size 15, an intermediary path of length 4, and each clique starting with either 10% or 90% cooperators. The different cliques are denoted by the differently colored and styled lines.

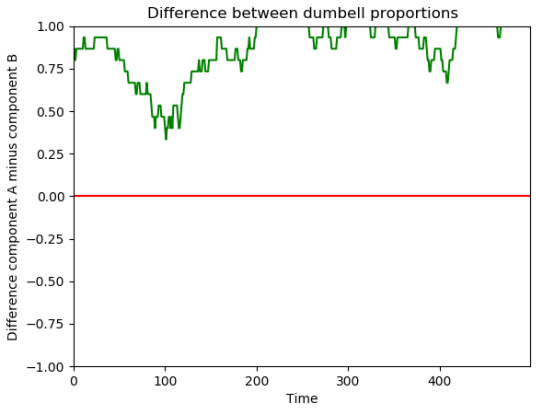

Figure 7: Difference in proportions of cooperators for a two-clique barbell graph with cliques of size 15, an intermediary path of length 4, and each clique starting with either 10% or 90% cooperators.

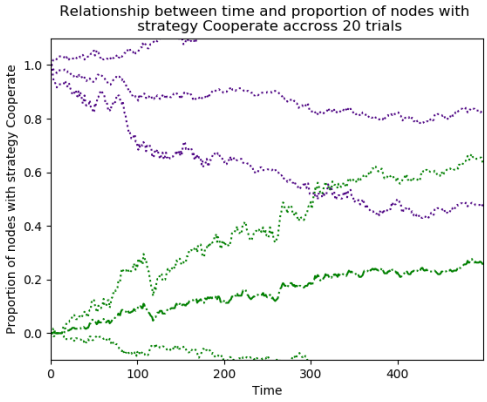

Figure 8: The average proportion of cooperators over time for each clique in a 2-barbell with cliques of size 15, an intermediary path of length 4, and each clique starting with either 10% or 90% cooperators. The different cliques are denoted by the differently colored and styled lines with their standard deviations drawn in the same color above and below.

3.2 Island graphs

A similar construction to the barbell graph is that of the island model, whose properties have been studied greatly by [4]. Note that for all simulations of island graphs we employ the *death-birth* model for strategy updating.

Definition 3.2. A **two-island graph** is a complete undirected graph with no self loops whose node set is separated into two disjoint sets: an island $\mathcal{A}$ and an island $\mathcal{B}$, such that the edges have the following weights:

- edges connecting two nodes in the same island have weight q
- edges connecting two nodes from different islands have weight m, with $m \ll 1$

The choice of edge weights directly affects the probability of two nodes interacting with each other. Indeed, it is much more likely for nodes in the same island to interact than for nodes in different islands. This structure has a similar behaviour to that of a barbell graph, in the sense that, when m is very close to zero, the impact of a node in a two island graph on a node from the opposite clique can be as small as it would be on a barbell graph with small path size.

Also, note that if $n_{\mathcal{A}}$ and $n_{\mathcal{B}}$ are the respective sizes of the islands $\mathcal{A}$ and $\mathcal{B}$, then the assumption that $n_{\mathcal{A}} = n_{\mathcal{B}} = N$ implies that the island is a weighted regular graph, namely that for every node $i \in \mathcal{G}$, the sum of its incident edge weights is $Nm + (N-1)q$. Let us name this homogeneous node weight ω, which will be useful in our theoretical discussion in Chapter 4.

We ran several simulations on two-island graphs in order to determine how strategies propagate through its structure. In figures 9 and 10, we see how, even when the starting proportions of cooperators are very different for each clique, eventually the proportions of cooperators in every clique converge.

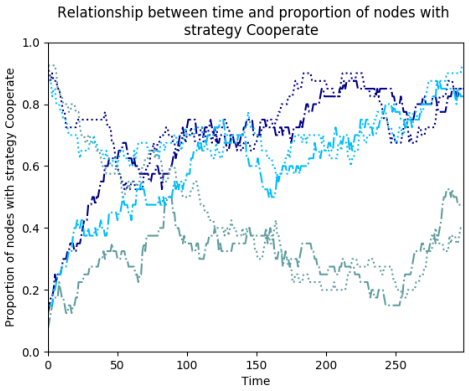

Figure 9: Two islands, starting with 20% and 80% of cooperators.

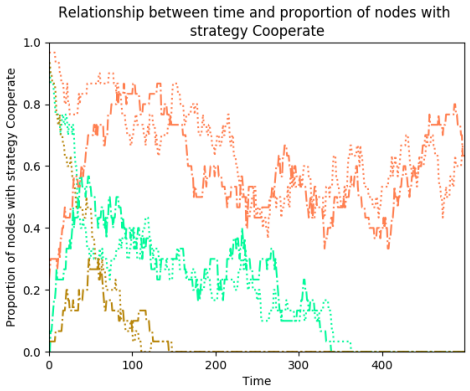

Figure 10: Two islands, starting with 10% and 90% of cooperators.

In figures 9 and 10, each color corresponds to a trial and each linestyle denotes one of the two islands. In all trials the graph starts out in a state where one clique has 20% cooperators and the other has 80% cooperators. As we can see in the above figure, over time the proportions of cooperators in each clique become equal for a given network. Note, however, that the exact proportion of cooperators that is reached differs for each trial.

We also ran simulations in which we averaged the proportion of cooperators in each of the cliques over more than one trial. In both simulations, all islands had 25 nodes and m, the weight of edges across cliques, was set as $m = 0.002$. We ran 50 trials for Figure 11, whereas we ran 20 trials for plotting the results in figure 12. As the reader can observe, the proportion of cooperators of both cliques becomes very close in the long term.

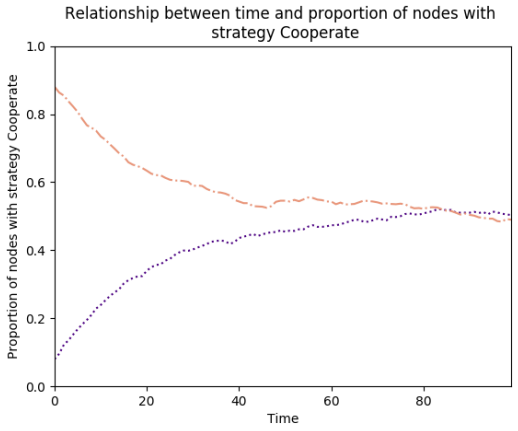

Figure 11: Two islands, starting with 10% and 90% of cooperators, respectively, over 50 trials, each of 100 timesteps.

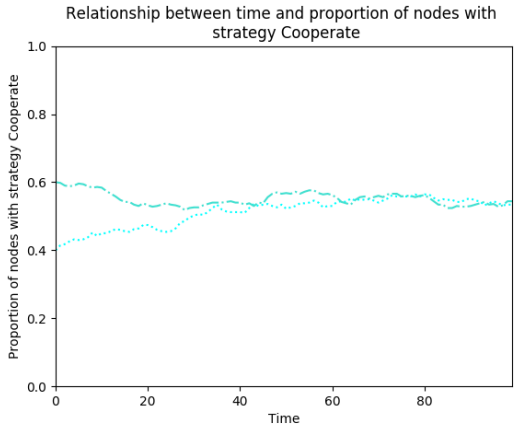

Figure 12: Two islands, starting with 40% and 60% of cooperators, respectively, over 50 trials, each of 100 timesteps.

3.3 Rich Club graphs

To further understand how the connectivity of graphs affects the propagation of cooperative strategies, we shall also examine rich club graphs. Just as above, there might be different definitions given for a rich club graph. This is, however, the definition that we worked with:

Definition 3.3. A **rich-club** graph is a complete, undirected graph with no self loops whose node set is separated into two groups: a *club* of size k_c and a periphery of size k_p, with $k_c \ll k_p$, such that the edges have the following weights:

- edges connecting two rich club nodes have weight a
- edges connecting a rich club node and a periphery node have weight b
- edges connecting two periphery nodes have weight c

Remark. In our simulations, we utilised values of c that were close to 0 and values of a that were close to 1. In particular, we used $c = 0.1$, $a = 0.9$ and $b = 0.5$.

In other words, these are extremely heterogeneous graphs constituted by a small dense core of highly weighted, highly connected nodes called the *rich club*, and a large yet sparsely-connected set of nodes called the *periphery*. This model can be very useful to represent certain networks like oligarchy institutions [4]. The reason why we were interested in this graph model was that it was basically an island model, but breaking the folloing two symmetries: (1) *size of graph* : our two clique sizes are now far apart from each other; (2) *connectivity within the cliques*: the rich club is densely connected whereas the periphery is sparsely connected.

The following images are the results from running Monte Carlo simulations on rich clubs. In all simulations of barbell graphs we employ the *death-birth* model for strategy updating. The left simulation has: $num\_trials = 1$; $t = 100$. The parameters varying across simulations are specified below:

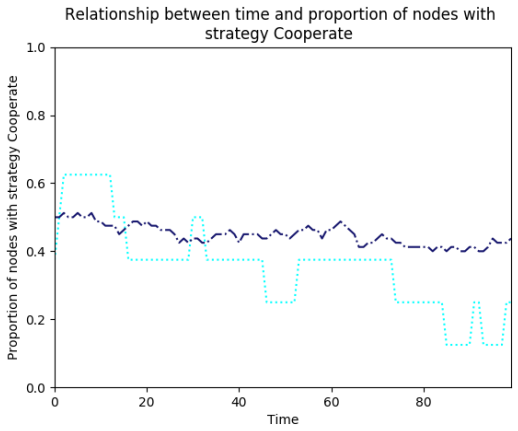

Figure 13: Club size $k_c = 8$; periphery size $k_p = 80$; $prop\_coop_{\text{rich}} = 0.4$; $prop\_coop_{\text{pphery}} = 0.5$

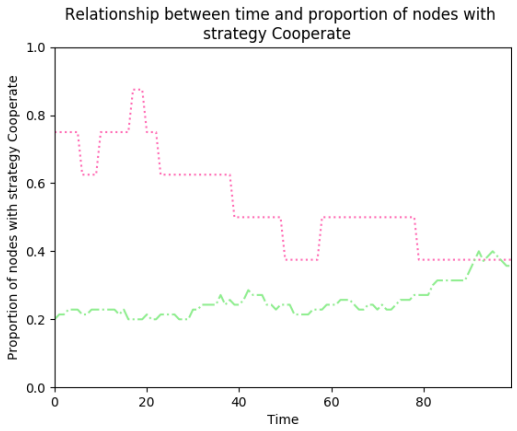

Figure 14: Club size $k_c = 8$; periphery size $k_p = 70$; $prop\_coop_{\text{rich}} = 0.7$; $prop\_coop_{\text{pphery}} = 0.2$

From our simulations, we can see that in rich-club graphs with these parameters there is a tendency for the proportions of cooperators in the rich-club and the periphery to converge in the long-term. In particular, the proportion of cooperators that is converged upon tends to be more similar to the starting proportion of cooperators in the periphery than that of the rich club.

A possible explanation for this may be that in these models the periphery nodes have connecting edge weights that are much stronger than those connecting the rich-club nodes or those connecting the rich-club and the periphery nodes. An area of further study would be to make differing choices for the parameters a, b, c ($a = 0.999$, $b = 0.8$ and $c = 0.001$ for instance), so that the influence of the periphery on the rich club would be less notorious.

4 Theoretical Results

Through running the aforementioned simulations and analyzing their empirical results, several patterns arose. The primary observation was that in all of the graph structures mentioned above the proportion of nodes with strategy *cooperate* in each of the given cliques (respective to their graph structure) converged after many time steps. This phenomenon, however, was not persistent in all the starting conditions of the two-barbell graph. Nevertheless, this phenomenon was prevalent in all the simulations performed on the island model. Therefore, we present the following proposition:

Proposition 4.1. *Given a two island graph consisting of two cliques $\mathcal{A}$ and $\mathcal{B}$, such that they have a starting proportion of cooperator nodes $C_A(0)$ and $C_{\mathcal{B}}(0)$ respectively,*

$$\lim_{t\to\infty} \mid C_{\mathcal{A}}(t) - C_{\mathcal{B}}(t) \mid = 0$$

While this observation has not been proved yet, we present in this section the work that we did in order to understand this phenomenon. In our calculations, we started by working with the following variables:

Variable name	Meaning
b	benefit that a cooperator bestows upon the other player
c	cost that a cooperator has to pay in order to help
s_i	the strategy of node i, either *cooperate* or *defect*
s	the string of random variable s_i, with $i \in \mathcal{G}$
$S(t)$	the string of node strategies at time t
δ	strength of selection
$w_{ij} = w_{ji}$	weight of an edge that connects i and j
$w_i = \sum_{j\in\mathcal{G}} w_{ij}$	node weights
$p_{ij} = w_{ij}/w_i$	probability of going from node i to node j in a random walk on $\mathcal{G}$, parametrized by edge weights
$\omega = \sum_{i\in\mathcal{G}} w_i$	the total node weight of the graph
$\pi_i = w_i/\omega$	the stationary probability of node i in a random walk on $\mathcal{G}$, parametrized by edge weights
$f_i(s)$	the edge-weighted average payoff of vertex i in state s
$F_i(s)$	the reproductive rate of vertex i in state s

Note that above, being able to define $S(t)$ implied that we are working in the continuous-time version of the evolutionary game consisting on the *death-birth* process, which, does not affect neither fixation probabilities, nor conditions for success [4]. We recall that $F_i(s) = 1 + \delta f_i(s)$, as well as the formula for $f_i(s)$, the edge-weighted average payoff of vertex i,

$$f_i(s) = -cs_i + b\sum_{j\in\mathcal{G}} p_{ij}s_j$$

We work on a two-clique island graph that is updated according to death birth model. Following the work of Allen et al. (2017) [4], and using all of the values stated above, we define a function $\overline{S}$ that describes the state of the graph. Unlike Allen's original model, however, we don't want to measure the number of cooperators, but the difference between the number of cooperators between the two cliques. We then label the two cliques as $\mathcal{A}$ and $\mathcal{B}$, and define the following variable:

$$\widetilde{\pi}_i = \begin{cases} \pi_i & \text{if } i \in \mathcal{A} \\ -\pi_i & \text{if } i \in \mathcal{B} \end{cases}$$

Which permits us to define $\overline{S}$ as

$$\overline{S} = \sum_{i\in\mathcal{G}} \widetilde{\pi}_i s_i$$

An important notion that was introduced in the supplementary notes of [4] was that of the expected instantaneous rate of change, which we can also use with $\overline{S}$:

$$\mathbb{E}\left[\overline{S}(t+\epsilon) - \overline{S}(t) \quad | \quad \overline{S}(t) = s\right] = D(\overline{s})\epsilon + o(\epsilon)$$

Note that, given that i replaces j, the change in $\overline{S}$ is $\widetilde{\pi}_j(s_i - s_j)$. We can then calculate the expected instantaneous rate of degree-weighted frequency change $D(\overline{s})$ [4] in the following way :

$$\begin{aligned} D(\overline{s}) &= \sum_{j\in G} \widetilde{\pi}_j \left(-s_j + \sum_{i\in G} s_i \frac{w_{ij}F_i(s)}{\sum_{k\in G} w_{kj}F_k(s)} \right) \\ &= \delta \left(\sum_{i\in G} s_i \left(0 + \sum_{j\in G} \left(\widetilde{\pi}_j p_{ji} f_i(s) - \widetilde{\pi}_j \sum_{k\in G} p_{jk}p_{ji}f_k(s) \right) \right) \right) + O(\delta^2) \\ &= \delta \left(\sum_{i\in G} s_i \sum_{j|j\sim i} \alpha_{ji}(s) + \sum_{i\in G} s_i \sum_{i|i\nsim j} \alpha_{ji}(s) \right) + O(\delta^2) \end{aligned}$$

Remark. Above, we use the following notation to denote an equivalence relation between members of the same clique: this is, $i \sim j$ denotes that i is in the same island as j and $i \nsim j$ denotes that i is not in the same island as j.

In order, we took the expectation of the change in $\overline{S}$ using $Rate[i \to j]$ from [4], then utilised a Taylor expansion around $\delta = 0$, and finally denoted

$$\alpha_{ji}(s) = \widetilde{\pi}_j p_{ij} f_i(s) - \widetilde{\pi}_j \sum_{k \in G} p_{jk} p_{ji} f_k(s)$$

In order to reduce the first term of $D(\overline{s})$, we do the following.

$$\begin{aligned}
\delta \sum_{i \in G} s_i \sum_{j|j\sim i} \alpha_{ji}(s) &= \delta \sum_{i \in G} s_i \left(\pi_i f_i(s) \sum_{j|j\sim i} p_{ij} - \sum_{j|j\sim i} \pi_i \sum_{k \in G} p_{ij} p_{jk} f_k(s) \right) \\
&= \delta \sum_{i \in G} s_i \left(\pi_i f_i(s) \sum_{j|j\sim i} p_{ij} - \pi_i \sum_{j|j\sim i} \sum_{k \in G} f_k(s) \sum_{j|j\sim i} p_{ij} p_{jk} \right) \\
&= \delta \sum_{i \in G} s_i \left((-\pi_i) f_i(s) \sum_{j|j\nsim i} p_{ij} - (-\pi_i) \sum_{j|j\nsim i} \sum_{k \in G} p_{ij} p_{jk} f_k(s) \right) \\
&= \delta \sum_{i \in G} s_i \left((-\pi_i) f_i(s) \sum_{j|j\nsim i} p_{ij} + \pi_i \sum_{k \in G} f_k(s) \sum_{j|j\nsim i} p_{ij} p_{jk} \right) \\
&= \delta \sum_{i \in G} s_i \left(\pi_i f_i(s) \left(\sum_{j|j\sim i} p_{ij} - \sum_{j|j\nsim i} p_{ij} \right) + \pi_i \sum_{k \in G} f_k(s) \left(- \sum_{j|j\sim i} p_{ij} p_{jk} + \sum_{j|j\nsim i} p_{ij} p_{jk} \right) \right) \\
&= \delta \sum_{i \in G} s_i \pi_i \left(f_i(s) \left(\frac{(N-1)q - Nm}{\omega} \right) + \sum_{k \in G} f_k(s) \left(- \sum_{j|j\sim i} p_{ij} p_{jk} + \sum_{j|j\nsim i} p_{ij} p_{jk} \right) \right)
\end{aligned}$$

where q denotes the edge weight between nodes in the same island and m denotes the edge weight between nodes in different islands. Now we focus on reducing $- \sum_{k \in G} f_k(s) \sum_{j|j\sim i} p_{ij} p_{jk} + \sum_{j|j\nsim i} p_{ij} p_{jk}$. By splitting up our summation according to which of the two islands k is in, we get the following:

$$- \sum_{k \in G} f_k(s) \left(\sum_{j|j\sim i} p_{ij} p_{jk} + \sum_{j|j\nsim i} p_{ij} p_{jk} \right) =$$

$$\left(- \sum_{j|j\sim i,\ j\sim k} f_k(s) p_{ij} p_{jk} \right) - \left(\sum_{j|j\sim i,\ j\nsim k} f_k(s) p_{ij} p_{jk} \right) + \left(\sum_{j|j\nsim i,\ j\sim k} f_k(s) p_{ij} p_{jk} \right) + \left(\sum_{j|j\nsim i,\ j\nsim k} f_k(s) p_{ij} p_{jk} \right) =$$

$$\left(- \sum_{j|j\sim i,\ j\sim k} f_k(s) \frac{q^2}{\omega^2} \right) - \left(\sum_{j|j\sim i,\ j\nsim k} f_k(s) \frac{qm}{\omega^2} \right) + \left(\sum_{j|j\nsim i,\ j\sim k} f_k(s) \frac{qm}{\omega^2} \right) + \left(\sum_{j|j\nsim i,\ j\nsim k} f_k(s) \frac{m^2}{\omega^2} \right).$$

Note that in the above equation we assumed $j \neq i$ and $j \neq k$, since our graphs have no self loops, and a factor $p_{ij} = 0$ or $p_{jk} = 0$ would imply that the corresponding summand is 0. In this last expression, the middle two terms sum to zero, due to the following: From the complete equation for $D(s)$, we can see that each i value is fixed

before we take the sums in the above expression. To further our analysis of the last equation term by term, let us assign the following σ_i values:

$$\sigma_1 = -\sum_{j|j\sim i,\ j\sim k} f_k(s)\frac{q^2}{\omega^2}$$
$$\sigma_2 = -\sum_{j|j\sim i,\ j\nsim k} f_k(s)\frac{qm}{\omega^2}$$
$$\sigma_3 = \sum_{j|j\nsim i,\ j\sim k} f_k(s)\frac{qm}{\omega^2}$$
$$\sigma_4 = \sum_{j|j\nsim i,\ j\nsim k} f_k(s)\frac{m^2}{\omega^2}.$$

In both σ_2 and σ_3 it is the case that $i \nsim k$. So we can rewrite the expression as the following:

$$\sigma_2 + \sigma_3 = \sum_{k|k\nsim i}\left(\sum_{j|j\sim k} f_k(s) - \sum_{j|j\nsim k} f_k(s)\right)$$

Supposing there are N nodes in each clique in our graph, there are $N-1$ values of j such that $j \sim k$ and $N-1$ values of j such that $j \nsim k$. The value of $f_k(s)$ does not depend on the position of j, so we have that

$$\sigma_2 + \sigma_3 = \sum_{k|k\nsim i}\Big((N-1)\cdot f_k(s) - (N-1)\cdot f_k(s)\Big) = \sum_{k|k\nsim i} 0 = 0$$

Therefore, the equation simplifies to

$$-\sum_{k\in G} f_k(s)\Big(\sum_{j|j\sim i} p_{ij}p_{jk} + \sum_{j|j\nsim i} p_{ij}p_{jk}\Big) = \sigma_1 + \sigma_4$$
$$= \Big(-\sum_{j|j\sim i,\ j\sim k} f_k(s)\frac{q^2}{\omega^2}\Big) + \Big(\sum_{j|j\nsim i,\ j\nsim k} f_k(s)\frac{m^2}{\omega^2}\Big)$$
$$= \sum_{k|k\sim i}\left(\left(\sum_{j|j\sim k} f_k(s)\cdot\frac{-q^2}{\omega^2}\right) + \left(\sum_{j|j\nsim k} f_k(s)\cdot\frac{m^2}{\omega^2}\right)\right)$$
$$= \sum_{k|k\sim i}\Big((N-2)\cdot f_k(s)\cdot\frac{q^2}{\omega^2} + (N)\cdot f_k(s)\cdot\frac{m^2}{\omega^2}\Big)$$
$$= \sum_{k|k\sim i} f_k(s)\cdot\frac{Nm^2-(N-2)q^2}{\omega^2}$$

Substituting this back into the full equation for $D(s)$ gives us

$$D(s) = \delta\sum_{i\in G} s_i\pi_i\left(f_i(s)\left(\frac{(N-1)q-Nm}{\omega}\right) + \sum_{k|k\sim i} f_k(s)\cdot\frac{Nm^2-(N-2)q^2}{\omega^2}\right)$$

Because $f_i(s) = -cs_i + b\sum_{j\in G} p_{ij}s_j$, then we know that $f_i(s)$ can be lower bounded $f_i(s) \leq b$ (in the case that i defects while all of its neighbors cooperate). Therefore,

$$\begin{aligned} D(s) &= \delta \sum_{i\in G} s_i\pi_i \left(f_i(s) \left(\frac{(N-1)q - Nm}{\omega} \right) + \sum_{k|k\sim i} f_k(s) \cdot \frac{Nm^2 - (N-2)q^2}{\omega^2} \right) \\ &\leq \delta \sum_{i\in G} s_i\pi_i \left(b \left(\frac{(N-1)q - Nm}{\omega} \right) + \sum_{k|k\sim i} b \cdot \frac{Nm^2 - (N-2)q^2}{\omega^2} \right) \\ &= \delta \sum_{i\in G} s_i\pi_i b \left(\frac{(N-1)q - Nm}{\omega} + \frac{N\cdot(Nm^2 - (N-2)q^2)}{\omega^2} \right) = \delta\Phi b \cdot \overline{S} \end{aligned}$$

Where $\Phi = \left(\frac{(N-1)q-Nm}{\omega} + \frac{N\cdot(Nm^2-(N-2)q^2)}{W^2} \right)$ is a constant. Similarly, we can observe the lower bound $-c \leq f_i(s)$ (the case where i is a cooperator and all of its neighbors defect), and then derive a similar result to the one above, so as to obtain these bounds:

$$\delta(-c\Phi \cdot \overline{S}) \leq D(\overline{S}) \leq \delta(b\Phi \cdot \overline{S})$$

Then, by assuming equality in both of the inequalities above, we obtain a differential equation with respect to δ. By solving it, we can then say:

$$\Omega(e^{-c\cdot\Phi\cdot\delta^2/2}) = \overline{S} = \mathcal{O}(e^{b\cdot\Phi\cdot\delta^2/2})$$

Upon arriving to this result, we were not able to conclude a proof for Proposition 4. However, working through these calculations was crucial for us to better understand the relationship of $D(\overline{S})$ and $\overline{S}$, and thus the long term difference of cooperators between two cliques in a two island model.

5 Discussion

The reasons behind why individuals sacrifice some of their own fitness in order to help their neighbors is not well understood by biologists. This is partly due to the enormous number of factors accounting for individuals' fitness levels and strategy updates. To further quantify and understand this phenomenon, we employed computer simulations to model large networks of nodes simultaneously interacting and updating their strategies. In particular, this project focused on the behaviour of *two-barbell* graphs, *two-island* graphs, and *rich-club* graphs, as the reader can observe in sections 3.1, 3.2, and 3.3, respectively.

In the case of the *two-island* model, we conjectured that this type of graph behaves in such a way that over time, the two cliques will come to have the same proportion of cooperators. This conjecture was supported by our computer simulations, as can be observed in **??**.

5.1 Future Work

Although this work focused on games having only two possible strategies, there are many other game variations yet to be explored. The behavior of complicated networks over long periods of time is still not fully understood, however the following areas of study may greatly help in shedding light on this complicated topic:

- Concluding the work done in order to prove Proposition 4.
- Developing faster algorithms so that the simulations take less time.
- Relating the phenomenon of decreasing frequency difference between islands discussed in section 6 with that of *thermal equilibrium*. Although models for thermal equilibrium are continuous and models in evolutionary game theory discrete, a possible way to do this might be to analyze strategy updating as a Poisson process.
- Simulating networks where different types of games are played on different areas of the graph. This could provide a more accurate model for real-world phenomenon, as often laws and trade rules differ according to geographical location.
- Incorporating the strategy *tit-for-tat*, which was mentioned in chapter 1, in the simulations, so as to make our model more realistic.

6 Acknowledgements

This paper was made during summer of 2018, as part of the Summer Program in Undergraduate Research (SPUR+) at Massachusetts Institute of Technology. We would like to thank the members of the MIT Mathematics Department for their support of this program, Prof. Slava Gerovitch, for directing this program, our mentor Ashwin Narayan, for his invaluable advice throughout the project, and our SPUR advisors, Prof. Ankur Moitra and Prof. Davesh Maulik, for their important guidance during each of our weekly meetings. We would also like to thank Bonnie Berger, for her advice on the topic, and Prof. Benjamin Allen, for having shared with us two papers which were central to our research and for his invaluable help with understanding some of his theoretical calculations. Finally, we would like to thank Kevin William Beuchot Castellanos, for encouraging and helping us to better understand previous work done with $D(S)$, Alejandro Vientós, for all his help in introducing us to the field of evolutionary game theory, and Timothy Ngotiaoco and Kavish Gandhi, for their much-appreciated guidance and help with writing this paper.

References

[1] B. Allen and M.A. Nowak. *Games on Graphs*. European Mathematical Society, 2015. ISBN: DOI 10.4171/EMSS/3. URL: http://www.ems-ph.org/journals/show_abstract.php?issn=2308-2151&vol=1&iss=1&rank=3.

[2] Babak Fotouhi et al. "Conjoining cooperative societies facilitates evolution of cooperation". In: *Nature Human Behavior* (July 2018), pp. 492–499.

[3] Adam D. I. Kramer, Jamie E. Guillory, and Jeffrey T. Hancock. "Experimental evidence of massive-scale emotional contagion through social networks". In: *Proceedings of the National Academy of Sciences* 111.24 (2014), pp. 8788–8790. ISSN: 0027-8424. DOI: 10.1073/pnas.1320040111. eprint: http://www.pnas.org/content/111/24/8788.full.pdf. URL: http://www.pnas.org/content/111/24/8788.

[4] Gabor Lippner et al. "Evolutionary dynamics on any population structure". In: *Macmillan Publishers Limited, Springer Nature* (Apr. 2017), p. 1.

[5] Martin. Nowak. "Evolving cooperation". In: *Journal of Theoretical Biology* 299 (Apr. 2012), pp. 1–8.

[6] Jorge M. Pacheco, F.C. Santos, and David Dingli. "The ecology of cancer from an evolutionary game theory perspective." In: *Interface Focus. Royal Society Publishing* (Apr. 2014), p. 1.

[7] Joirgen W. Weibull. *Evolutionary Game Theory*. The MIT Press, 1995.

[8] Ned S. Wingreen and Simon A. Levin. "Cooperation among Microorganisms". In: *PLoS Biology* (9 Sept. 2006), p. 1487.